Numerical tests of constitutive laws for dense granular flows

Gregg Lois,[1] Anaël Lemaître,[1,2] and Jean M. Carlson[1]
[1]*Department of Physics, University of California, Santa Barbara, California 93106, USA*
[2]*LMDH-Universite Paris VI, UMR 7603, 4 place Jussieu, case 86, 75005 Paris, France*
(Received 21 January 2005; revised manuscript received 7 June 2005; published 14 November 2005)

We numerically and theoretically study the macroscopic properties of dense, sheared granular materials. In this process we first consider an invariance in Newton's equations, explain how it leads to Bagnold's scaling, and discuss how it relates to the dynamics of granular temperature. Next we implement numerical simulations of granular materials in two different geometries—simple shear and flow down an incline—and show that measurements can be extrapolated from one geometry to the other. Then we observe nonaffine rearrangements of clusters of grains in response to shear strain and show that fundamental observations, which served as a basis for the shear transformation zone (STZ) theory of amorphous solids [M. L. Falk and J. S. Langer, Phys. Rev. E. **57**, 7192 (1998); M.R.S. Bull **25**, 40 (2000)], can be reproduced in granular materials. Finally we present constitutive equations for granular materials as proposed by Lemaître [Phys. Rev. Lett. **89**, 064303 (2002)], based on the dynamics of granular temperature and STZ theory, and show that they match remarkably well with our numerical data from both geometries.

DOI: 10.1103/PhysRevE.72.051303 PACS number(s): 81.05.Rm, 83.50.−v, 62.20.Fe, 83.10.Gr

I. INTRODUCTION

Historically reserved to the engineering community [1–4], granular materials recently emerged as a new field of study for physicists [5–11]: a state of matter that is not classifiable according to the traditional ternary—solid, liquid, or gas—and requires scientists to rethink the foundations of statistical physics and thermodynamics [12,13]. The first theories of granular materials were motivated primarily by the need to predict the creep motion of soils and their stability properties. Inspired by continuum theories of plasticity, these approaches were restricted to quasistatic deformation and incipient failure [1–4,14–16]. In physics, initial progress came in understanding dilute granular materials with the development of kinetic theory [17–29]. But kinetic theory is based on the assumption that interactions between grains occur during instantaneous binary collisions, a condition that is expected to break down in the dense regime.

Traditional approaches thus leave us with little understanding of the elementary mechanisms of deformation in dense granular materials. It is no wonder that the elaboration of physically inspired constitutive equations for granular materials is currently facing a collection of controversial issues which challenge its basic assumptions. Common points of contention include (i) the relevant features of the grain-grain interaction—e.g., Hertzian versus hard-sphere repulsion [11,30,31]—(ii) the domain of applicability of kinetic theories [26,28,32–34], (iii) the observation and micromechanical origin of Bagnold scaling in dense flows [35–40], and (iv) the plausible need to formulate "nonlocal" constitutive equations [41–45] due to the existence of force chains [46–50]. Uncertainties about these questions have fueled a wealth of theoretical models. Some models posit that frustrated rotation plays a preeminent role in jamming [51,52]. Many models propose extensions of kinetic theory by using either granular temperature [53], introducing strongly density-dependent viscosities [54–56], or incorporating a quasistatic stress at the internal friction angle of the material [57–62]. Other models are based on the introduction of force chains [41–43], activated processes [63], "granular eddies" [44], coexisting liquid and solid microphases in a Ginzburg-Landau formulation [64–66], or "spots" of free volume associated with cooperative diffusion [67,68].

Several of the above-mentioned models conjecture jamming mechanisms—frustrated rotations, force chains, granular eddies—which are so specific to granular materials that they do not allow direct connections with jamming in other materials. Our approach rests on the viewpoint that, since jamming is observed in many amorphous systems, it is likely that it has a common origin. It was thus proposed [69] that a rescaling of the dynamics of perfectly hard granular materials would make it possible to map their properties onto more typical glass formers. Building on the analogy between granular materials and metallic glasses then provides a local mechanism of jamming on the basis of the shear transformation zone (STZ) theory of plasticity [70,71].

The goal of the present paper is to both discuss some of the microscopic assumptions underlying the construction of constitutive equations for granular materials and test some specific predictions of the STZ theory formulation of such equations [69]. Our approach is based on the following expectations concerning the four points of contention identified above: (i) major properties of dense granular flows can be captured by perfectly hard grains; (ii) jamming is associated with changes in the contribution of long-lasting contacts to the stress tensor, in regimes where the collisional contributions—those predicted by kinetic theory—are negligible; (iii) for flows of perfectly hard grains, Bagnold's scaling is relevant at all densities in the bulk of the flow and arises from an invariance in the equations of motion; and (iv) the rheology of dense granular materials is local in a sense to be defined further.

Indeed, (i) a recent work by Campbell has shown—convincingly to us—that most natural and experimental flows occur in a regime of strain rates where grains can be considered as hard spheres [72]. Although this question may

still be debated, we will take this for granted and restrict our study to a material composed of perfectly hard grains. (ii) The breakdown of kinetic theory in dense flows has now been characterized in several numerical and experimental studies [73–78] and indicates that jamming is associated with changes in the contribution of long-lasting contacts to the stress tensor, not the collisional contribution. We will take this idea for granted in the present work, but we do believe that a quantitative analysis of this statement is needed and will devote a future paper to this question [79]. (iii) We will show following [69] that in the case of perfectly hard grains Bagnold's scaling holds for any density, in the bulk of the flow. Assumption (iv) is strongly inspired by the works by Aranson and co-workers, who have shown that a Ginzburg-Landau formulation of a fluid-solid mixture [64–66] could account for important properties of granular flows. This suggests that a local formulation of granular rheology, coupled to hydrodynamic equations, can be sufficient to account for a large part of the phenomena observed in dense granular flows. However, no numerical study has been specifically devoted to the question of whether constitutive equations that hold in one shearing geometry will also hold in a different shearing geometry, with the same fitting parameters. This is closely related to the notion of locality and whether boundary effects play a role in bulk dynamics.

Therefore, we will first study whether dense granular flows can be described as a local phenomenon, governed by local continuum equations, or whether granular flows must be treated nonlocally, relying on the emergence of long-range correlations through microscopic mechanisms such as force chains. For this purpose we have implemented contact dynamics simulations of sheared granular materials in two different configurations: (i) simple shear in a periodic cell and (ii) thick flows of granular material down an incline plane. We will show that the measurements obtained in either configuration can be extrapolated to the other.

Next we follow Falk and Langer [70,71] and test for the consistency of the STZ picture of material deformation advocated by these authors. Our observation provides further support for the analogy between granular materials and common glass formers and direct support for the relevance of STZ theory to granular materials. A review of the STZ constitutive equations for granular flows will follow and finally a fit of the theory with our numerical data.

The organization of our paper is as follows. In Sec. II we present equations of motion in the mathematical limit of perfectly hard grains. We discuss the invariance properties of the equations of motion and how these properties are related to Bagnold's scaling. We also discuss why the results for perfectly hard grains are applicable to natural and experimental granular materials. In Sec. III we construct our numerical test, provide algorithmic details on the contact dynamics method, and compare the rheology of a dense granular materials in a periodic cell and down an incline plane. Finally, in Sec. IV, we present Falk and Langer's STZ theory, show how it adapts to granular materials, and conclude with fits of our data.

II. FUNDAMENTAL RESULTS FOR PERFECTLY HARD GRAINS

When grains are dry—so that no water bridges induce attraction—and of size larger than the micrometer scale—so that no electrostatic interaction intervenes—their interaction is purely repulsive. The interaction results from the elastic deformation of grains at contact and the dissipation of energy via friction and collisions. The complexity of this interaction motivates our first question: which properties of the grain-grain interaction contribute to any particular macroscopic observation? In some instances, details of the grain-grain interaction seem critical: for example, the Hertzian repulsion [30] is essential to understand the acoustic properties of granular materials [80,81]. Numerical implementations of granular materials have thus relied on more or less elaborate models of the grain-grain interaction [82,83].

Here we are concerned with dense flows of granular materials and, in particular, flows down inclines as found in the experiments by Pouliquen [84] and numerics by Silbert and co-workers [38,39]. For these dense granular flows a recent study by Campbell helps us assess the importance of the elastic (soft) part of the repulsive potential [72] versus the limit in which grains appear as perfectly hard spheres. Campbell presented a detailed analysis of the different flow regimes obtained in a three-dimensional simple shear simulation of dense granular flows when varying the stiffness k of the repulsion, the shear rate $\dot{\gamma}$, and the mass density ϕ. He found that the dimensionless parameter $\Upsilon \equiv k/\phi D^3 \dot{\gamma}^2$, where D is the grain size, dictates the character of the flow. This quantity is directly related to a Mach number which involves the ratio of the shear velocity $D\dot{\gamma}$ over the sound speed c_s: $M = D\dot{\gamma}/c_s = 1/\sqrt{\Upsilon}$. The hard-sphere limit corresponds to the situation where sound waves travel very fast compared to the motion induced by the shear flow. This is the limit of very small Mach number, or small shear rates. Specifically, in the numerics by Campbell, this limit is reached for Mach numbers below $\sim 10^{-2}$. Since the sound speed in granular materials is of the order of 100 m/s, if we assume a grain size of the order of 1 mm, the Mach number is expressible as $M = 10^{-5}\dot{\gamma}$. Therefore, in order to be in the limit where grains behave as if they are perfectly stiff, it suffices to restrict oneself to shear rates below 1000 s^{-1}. Most experimental and natural situations occur at shear rates far below this limiting value, and we can conclude that most flows of grains are in the limit where the soft part of the repulsion is entirely masked by the steric exclusion. To study these flows it is sufficient to consider properties of perfectly hard grains. In the following sections we explore how the mathematical limit of perfectly hard spheres gives insight into fundamental processes which relate to many experimental shear flows.

A. Equations of motion and hard-sphere conditions

The motion of N spherical grains in a d-dimensional granular material is determined by Newton's equations for the positions q_i, angular orientations θ_i, momenta p_i, and angular velocities ω_i:

$$\frac{dq_i}{dt} = \frac{p_i}{m_i}, \quad \frac{dp_i}{dt} = \sum_j F_{ij} + F^{ext}, \tag{1}$$

$$\frac{d\theta_i}{dt} = \omega_i, \quad \frac{d\omega_i}{dt} = \frac{1}{I_i}\sum_j R_i \hat{n}_{ij} \times F_{ij}, \tag{2}$$

where F^{ext} represents an external force such as gravity, F_{ij} represents a contact force on grain i by grain j, $\hat{n}_{ij}$ is the unit normal vector pointing from grain i to grain j, R_i is the radius of grain i, and I_i is the moment of inertia.

These equations must be complemented with a prescription for the contact forces. In the hard-sphere limit these contact forces are determined self-consistently by the conditions that (i) there is no penetration between grain—a force is instantaneously created upon contact to impede penetration and remains nonzero until the contact is broken—and (ii) by the friction law which couples to rotational degrees of freedom.

Important properties of granular materials arise directly from an invariance of the equations of motion (1) and (2). We now spend some time studying these properties and assessing their consequences for macroscopic observations, in particular Bagnold's scaling.

B. Bagnold's scaling

The success of kinetic theory came in a large part from its ability to account for the scaling between stress σ and strain rate $\dot{\gamma}$ ($\sigma \sim \dot{\gamma}^2$) first observed by Bagnold in dense granular materials [35]. Bagnold justified this behavior with a simple argument: the frequency of collisions and momentum change per collision are each proportional to the shear rate and therefore the stress is proportional to the square of the shear rate. Similar dimensional arguments are also a part of kinetic theory and are closely related to the concept of granular temperature (see [85] for a review). However, since these arguments are only generally discussed in the framework of kinetic theory, it is unclear why Bagnold's scaling should hold in dense systems where grains do not interact solely through binary collisions.

This has led to a great deal of interest in the origin and existence of Bagnold's scaling for *dense* granular flows. On the one hand, Bagnold's observations have been criticized: they may have arisen from a secondary instability of the granular flow in his shear cell [37]. On the other hand, Bagnold's scaling has been directly observed by measuring shear stress and strain rate profiles in numerical simulations of granular flows down inclines [38,39] and is found to be consistent with experimental observations of the average flow rate in the same geometry [84]. The idea that dimensional invariance would hold for dense flows and enforce Bagnold's scaling has recently emerged [45,69].

We wish to highlight the fact that, far from being reserved to "rapid" flows where kinetic theory applies, this dimensional invariance is a profound property of Newton's equations for hard-sphere systems. It holds in both the dense and "rapid" flow regimes and does not require any of the assumptions of kinetic theory to hold. To clarify this issue, we find it useful to characterize the invariance in terms of phase-space trajectories: this picture is well adapted to the case of dense flows where grains undergo multibody interactions.

Namely, for a granular material free from external forces with a constant shear rate, the time evolution will obey Eqs. (1) and (2) with $F^{ext}=0$. If we now rescale the contact forces by a scalar value $F_{ij} \to F_{ij}/A$ and simultaneously rescale the time $t \to t\sqrt{A}$, then Newton's equations are transformed to read

$$\frac{dq_i}{dt} = \frac{p_i^{new}}{m_i}, \quad \frac{dp_i^{new}}{dt} = \sum_j F_{ij}, \tag{3}$$

$$\frac{d\theta_i}{dt} = \omega_i^{new}, \quad \frac{d\omega_i^{new}}{dt} = \frac{1}{I_i}\sum_j R_i \hat{n}_{ij} \times F_{ij}, \tag{4}$$

where $p_i^{new} = p_i/\sqrt{A}$ and $\omega_i^{new} = \omega_i/\sqrt{A}$. This form for Newton's equations is identical to Eqs. (1) and (2) with new values for the momenta and angular velocities.

Under the rescaling of contact forces and time, the positions and angular orientations remain unchanged, while the velocities are changed in accordance with the time rescaling. If we were to watch a movie of one granular flow where the grains have initial velocities p_i and ω_i and watch another movie at half the speed where the initial velocities are doubled, $p_i \to 2p_i$ and $\omega_i \to 2\omega_i$, the two movies would look exactly the same in the hard-sphere limit. The difference in the dynamics is that the contact forces measured in the second movie would be 4 times larger than those in the first.

This invariance is a property of *perfectly hard grains* which must hold in the inertial regime. This includes the regime infinitely close to jamming, where multibody interactions dominate collisional terms and the basic assumptions of kinetic theory fail. This invariance holds for any value of the restitution and friction coefficients. In an experiment, this scaling breaks down only when it is no longer appropriate to model the experimental system by perfectly hard grains. Relying on the arguments of Campbell introduced earlier [72], we can conclude that many experimental granular flows are in the regime where it is appropriate to model the system by hard grains.

Let us note that this invariance is not limited to translationally invariant situations, like in the bulk of a granular flow or a biperiodic simulation cell. Indeed, suppose that we study the motion of perfectly hard grains sheared between two confining walls taken themselves to be perfectly hard. Then, again, a rescaling of force and time scales leave the phase-space trajectories invariant. In other words, changing the shear rate imposed via the walls leaves the velocity profile of the confined granular medium—including possible boundary layers—invariant after the appropriate rescaling. The forces in the whole system are rescaled accordingly.

C. What quasistatic limit?

In amorphous systems such as low-temperature molecular glasses, dense suspensions, and foams, energy dissipation has a characteristic time scale. In these systems, as the strain rate is lowered *at constant density*, the strain rate may eventually become low compared to the dissipation rate. Then, the flow reaches a state where kinetic energy becomes negligible compared to other forms of energy and the material flow properties become independent of strain rate: this is the quasistatic regime. The situation is quite different for granu-

lar materials, as long as they can be modeled as perfectly hard grains, because the rate of energy dissipation scales with the strain rate. The terms entering Newton's equations always remain in the same ratio, which is a function of density only.

The quasistatic limit is thus pathological for perfectly hard grains: when the strain rate is scaled down, the system is always exploring the same trajectories in phase space, but at a slower speed.[1] In other words, the material cannot jam by lowering the strain rate; jamming is reached only by increasing the density [86].

This property suggests that it is essential to correctly account for the rate of elementary events which governs the microscopic dynamics—e.g., dissipation—in a dense granular flow. In dilute flows, the rate of elementary events is the rate of binary collisions. In dense flows, this notion should thus be generalized in terms of a "rate of elementary events."

D. Granular temperature

The above-mentioned invariance may help us form a picture for the physical interpretation of elementary events in dense flows. Under a simultaneous change in time and force scales, the positions and angular orientations of grains are invariant: the path that a granular material takes in configuration space is also invariant, and only the speed along this path is altered. Therefore, the path that a granular material takes in configuration space can be separated from the rate at which events occur along that path.

From a more physical standpoint, a dense granular flow of perfectly hard grains is animated with intense rattling and changes of the contact network orientation. The dynamics of the system involves many minute events which generalize binary collisions: these are, creation and opening of contacts, rearrangements of the existing force network, and sudden changes in the nature of a frictional contact (sliding or not). In our simulations, these events occur at a high frequency compared to the evolution of mean-field quantities. Hence we will assume that the frequency of microscopic events is a self-averaging quantity which can be given a mean-field value at the slow scale of the evolution of mean-field quantities in a dense system. We will *define* granular temperature T by denoting the frequency of microscopic events as $\sqrt{T}/\langle R\rangle$ (the average grain size $\langle R\rangle$ is inserted so that T has units of velocity squared).

This definition of "granular temperature" being given, we then notice that the kinetic energy should be proportional to T up to a density-dependent factor. The kinetic energy of a dense flow can be written as

$$T_k = \frac{m}{2}(\langle v^2\rangle - \langle v\rangle^2) + \frac{\langle I\rangle}{2}(\langle \omega^2\rangle - \langle \omega\rangle^2), \tag{5}$$

where m is the average mass, v the velocity, I the moment of inertia, ω the angular velocity, and brackets denote an average over grains. As we will focus on scalings which arise at constant density, we will neglect all density-dependent factors in the following constitutive equations and assume T is proportional to T_k in the present work. This means that at any time, the kinetic energy provides an estimate of the frequency of elementary events in a multicontact system.

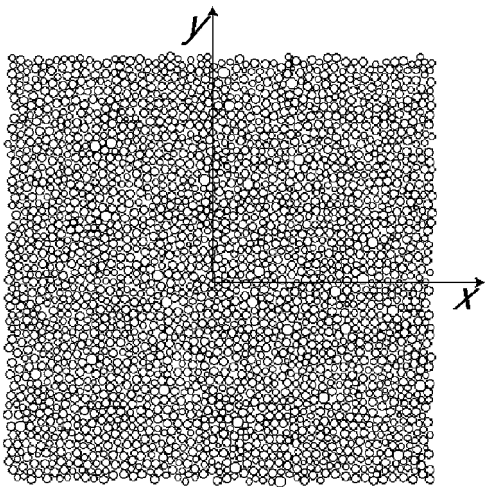

FIG. 1. Snapshot of a granular material simulation in the simple shear configuration. Each grain has an average velocity in the x direction given by $\dot{\gamma}y$, where $\dot{\gamma}$ is the strain rate. The center of the cell is defined as $x=y=0$.

Denote p as the pressure, σ the shear stress, $\dot{\gamma}$ the strain rate, ϕ the mass density, and D the average diameter of grains. Some important invariant (and dimensionless) quantities are $p/\phi D^2\dot{\gamma}^2$, $\sigma/\phi D^2\dot{\gamma}^2$, pD^d/T_k, $\sigma D^d/T_k$, $T_k/\phi D^{d+2}\dot{\gamma}^2$, and σ/p. These must be single-valued functions of *density* only (independent of the strain rate). This observation, established by the invariance in Newton's equations which holds for granular flows in the dense and collisional regimes, automatically predicts Bagnold's scaling: since $\sigma/\phi D^2\dot{\gamma}^2$ is a function of density only, it follows that $\sigma \propto \dot{\gamma}^2$.

III. CONSTRUCTION OF A NUMERICAL TEST

In constructing a numerical test our goals are to measure stress-strain relations when granular temperature and stresses are appropriately scaled, show that they compare well with the standard response of yield stress liquids, and show that the rheology measured in simple shear flow matches the bulk rheology of a granular flow down an incline.

In order to address these issues, we implement numerical simulations of granular materials in two different geometries.

(i) We implement simple shear flow in a cell with Lees-Edwards (LE) boundary conditions. In this configuration, the density and shear rate is prescribed and the simulation cell is, by construction, translationally invariant. This grants direct access to averaged quantities of the granular temperature and stress tensor. Using this configuration we can characterize the steady-state relation between stresses, granular temperature, and strain rate and extract numerically the parameters of a constitutive law for granular materials. A screenshot of this shearing geometry is shown in Fig. 1.

[1]This scaling property is directly related to the observation by Campbell that "there is no path between inertial (rapid) flow and quasistatic flow by varying the shear rate at fixed concentration" [72].

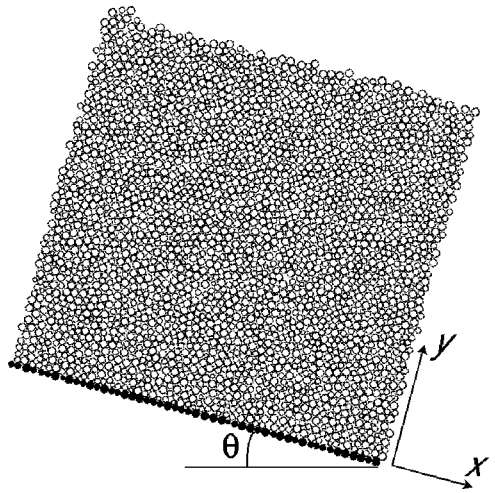

FIG. 2. Snapshot of a granular material simulation in the incline flow configuration. Fixed grains (indicated by solid circles) create a stationary incline at angle θ on which the flowing grains are accumulated and allowed to flow. Gravity drives the motion and is directed vertically downward.

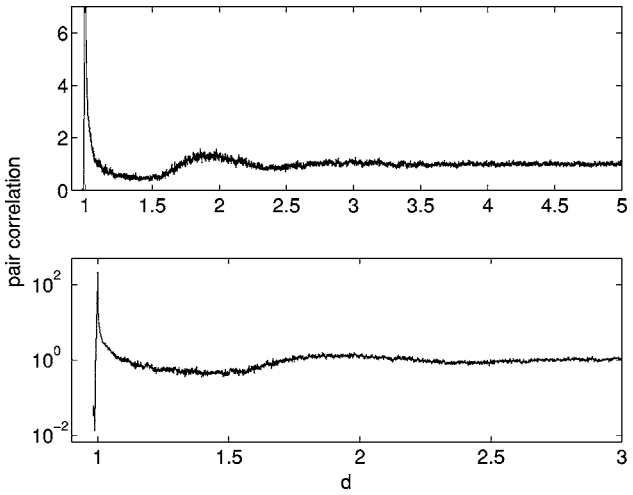

FIG. 3. The pair correlation function for a frictionless granular material at high density in linear (top) and logarithmic (bottom) scales, as a function of grain diameters d. This function is representative of the pair correlation functions for other densities and for granular materials with friction between grains. There is a large peak corresponding to contacting grains ($d=1$) and some variation between $d=1$ and $d=3$. For $d>3$ there is no correlation between grains. This implies that the material is amorphous.

(ii) We implement granular flow down an inclined plane made of stationary grains. The simulation cell is periodic in the direction (x) parallel to the plane and the flow is inhomogeneous in the perpendicular (y) direction. In this configuration, the stresses are prescribed by the angle of the incline. We perform x-averaged, y-dependent measurements of granular temperature, velocity profiles, and strain rate. Large heights of the granular layer grant access to the bulk rheology of the flow. This permits us to check the existence of a well-defined bulk rheology in the large-height limit and to compare it with the measurements in simple shear. A picture of this shearing geometry is shown in Fig. 2.

In order to make a quantitative comparison of the two simulations, we use the same material: a two-dimensional polydisperse mixture of constant-density grains with the radii drawn from a flat distribution with average radius $\langle R\rangle$ and width δR. For all of the simulations in this paper we set $\delta R/\langle R\rangle=0.5$, using $\langle R\rangle=0.7$. This distribution prevents crystallization and produces an amorphous granular material, as can be seen from measurement of the pair correlation function in Fig. 3. The horizontal axis (d) in this figure corresponds to the distance between a pair of grains, divided by the sum of their radii. This normalizes the figure so that $d=1$ corresponds to contacting grains. Other than this peak, the function has some small variation (which implies a correlation) between $d=1$ and $d=3$. However, there is no correlation beyond $d=3$. Because there is no large-scale correlation, this implies that the granular material is amorphous.

In this paper we present data for normal and tangential coefficients of restitution given by $e_n=e_t=0$ [see Eq. (6) for a precise definition of these coefficients]. It was shown by Chevoir *et al.* [87] that the regimes reached by granular materials are almost independent of the restitution coefficients below some threshold around $e_n=0.7$. Different friction coefficient have been used: frictionless grains and $\mu=0.4$.

Our simulations of granular materials rely on the contact dynamics algorithm [88–92]. In our case, where we are interested in the properties of perfectly rigid grains, the contact dynamics algorithm offers considerable advantage over a soft-sphere simulation [46]. By using the contact dynamics algorithm we will never be in a state where the deformation of grains determines the properties of the macroscopic flow. In particular this will allow us to demonstrate that the bulk properties of incline flow, which our study finds to be identical to those from previous studies [38,39], can be determined simply by considering properties of perfectly hard grains. Additionally, in the limit of high inelasticity and hard spheres, the contact dynamics algorithm is computationally faster than soft-sphere simulations, where the simulation time step scales inversely with both the particle stiffness and normal coefficient of restitution [93]. We refer to the literature for technical details of the contact dynamics algorithm and present below a brief overview of the method, supplemented by a single addition we made in order to construct a Lees-Edwards simulation cell for frictional granular materials.

A. Contact dynamics

A contact dynamics algorithm was constructed to carry out numerical simulation of spheres interacting through the enforcement of hard-sphere conditions [88].

When a contact occurs there is an noncontinuous force created that prevents the contacting grains from penetrating. The magnitude of this force is chosen to ensure that the final relative velocity u of the grains is related to the initial relative velocity u^0 via the equations

$$u_n=-e_n u_n^0, \quad u_t=e_t u_t^0, \tag{6}$$

where e_n and e_t are constant restitution coefficients that will depend on the shape and consistency of the grains, and the n

and t subscripts represent the normal and tangential parts of the relative velocity with respect to the contact. At each time step, the algorithm computes the contact forces by first ensuring that these relations hold at each contact.

To include friction, the contact dynamics algorithm ensures that the resulting tangential force F_t is less than or equal to μF_n where μ is the friction coefficient between grains and F_n is the normal force. If this constraint does not hold, then the algorithm sets $F_t = \mu F_n$ in order to comply with Coulomb friction.

In this way the contact dynamics algorithm calculates, at each time step, contact forces that are consistent with Newton's equations and the hard-sphere contact law.

B. Sllod equations for simple shear flow

Lees-Edwards boundary conditions permit us to prescribe the deformation of a material by controlling the positions of the image cells [94]. In all of the simulations presented here, we impose a constant strain rate $\dot\gamma$ so that a grain at position y has an average velocity of $\dot\gamma y$ in the x direction (see Fig. 1).

It was recognized in early implementations of LE boundary conditions that when deformation is applied through the image cells, the information needs time to propagate from the cell boundaries to its center. In order to ensure rapid propagation of this information and prevent the boundaries between cells from making unphysical contributions to the motion, it is necessary to modify Newton's equations by introducing so-called Sllod terms. These terms can be understood as a sort of "shear bath," with all particles in the cell being directly coupled to the overall deformation [95]. In practice, the Sllod terms introduce a mechanical perturbation to the equations of motion that gives each grain an average velocity consistent with simple shear flow. If we separate the momentum p_i of each grain i into the average part $m_i \dot\gamma y_i$ and fluctuating part $\tilde p_i$, so that $p_i = m\dot\gamma y_i + \tilde p_i$, then the Sllod equations read

$$\frac{dq_i}{dt} = \frac{\tilde p_i}{m_i} + \hat x \dot\gamma (q_i \cdot \hat y), \quad \frac{d\tilde p_i}{dt} = \sum_j F_{ij} - \hat x \dot\gamma (\tilde p_i \cdot \hat y). \tag{7}$$

The equation for the position q_i is simply the result of writing the momentum in terms of an average and fluctuating part. The equation for $\tilde p_i$ contains a new term $\hat x \dot\gamma (\tilde p_i \cdot \hat y)$ which forces the shear flow. Since every grain in the primitive cell is acted upon by this mechanical force, the constant strain rate is imposed on all of the grains simultaneously at the beginning of the simulation. This can be easily appreciated by writing the equations of motion (7) in terms of just the position. This yields

$$\frac{d^2 q_i}{dt^2} = \frac{1}{m_i}\sum_j F_{ij} + \hat x \frac{d\dot\gamma}{dt}(q_i \cdot \hat y), \tag{8}$$

where the equation of motion is only altered by including a term with the time derivative of the shear rate. In this paper, where we only consider simple shear flow simulations with a constant shear rate, the new term will be nonzero just at the beginning of the simulation. At this time it will serve to set the initial velocities of the grains such that $p_i = m\dot\gamma y_i$. After this initial intrusion, the new term will always be zero and the shear flow will be upheld by the LE boundary conditions. Furthermore, it can be proven that, in the LE geometry, the Sllod equations give an exact representation of simple shear flow arbitrarily far from equilibrium [95,96].

For a granular material with nonzero friction coefficient μ, the equations of motions should incorporate rotations of the grains (for $\mu = 0$ the tangential contact force is always zero and there is no rotation). It is expected that a Sllod term should arise in the equations of motion for the angular velocity since, in the linear velocity profile indicative of simple shear flow, the top and bottom of every grain should be moving with slightly different velocities. This will give each grain an average rotation of $\dot\gamma/2$ which must be incorporated in Eq. (2) just as the average velocity $\hat x \dot\gamma (q_i \cdot \hat y)$ was incorporated in Eq. (7). This leads to the following equations:

$$\frac{d\theta_i}{dt} = \tilde\omega_i + \frac{\dot\gamma}{2}, \quad \frac{d\tilde\omega_i}{dt} = \frac{2}{m_i r_i^2}\sum_j R_i \hat n_{ij} \times F_{ij}, \tag{9}$$

where $\tilde\omega_i$ denotes the fluctuating part of the angular velocity and we have inserted the moment of inertia of constant density disks in two dimensions.

Equations (7) and (9) now give an exact representation of simple shear flow for a frictional granular material arbitrarily far from equilibrium.

The primary interest of this procedure is that it permits us to simulate a sheared granular material with a homogeneous shear rate. Experimental procedures—e.g., in a Couette cell—do not guarantee that the strain rate is homogeneous: the existence of walls induces a nonuniformity of the flow and possibly localization of the deformation. Our protocol grants direct access to the rheology of the granular material in a self-averaging situation.

C. Macroscopic quantities

We define the stress tensor $\Sigma^{\alpha\beta}$ via Cauchy's equation

$$\phi \frac{d}{dt}\langle v^\alpha \rangle + \phi \langle v^\beta \rangle \partial_\beta \langle v^\alpha \rangle = -\partial_\beta \Sigma^{\alpha\beta} + f_{ext}^\alpha, \tag{10}$$

where $\langle v^\alpha \rangle$ is the average velocity in the α direction (averaged over all grains), ϕ is the mass density, and f_{ext} is the external force per volume. This equation simply states that the total time derivative of the average velocity (left-hand side) is proportional to the divergence of the stress tensor, plus any external forces. Cauchy's equation gives a definition of the stress tensor from which there exists a procedure to derive the functional form of the stress tensor. This is called the Irving-Kirkwood derivation [96], and it yields

$$\Sigma^{\alpha\beta} V = \sum_i m_i \tilde v_i^\alpha \tilde v_i^\beta + \sum_{i>j} (R_i + R_j) \hat n_{ij}^\alpha F_{ij}^\beta, \tag{11}$$

where $\tilde v_i$ is the fluctuating velocity of grain i determined by $\tilde v_i^\alpha = v_i^\alpha - \langle v_i^\alpha \rangle$, and V is the volume of the granular material (or area in two dimensions). In this paper we will focus on time- and space-averaged measurements of the stress tensor so that the Irving-Kirkwood formula is applicable. Other formulas must be applied when less-coarse-grained measurements are required [97,98].

The symmetric stress tensor can be written in terms of three variables: the pressure p, shear stress σ, and first normal stress difference N_1 defined as

$$\Sigma^{\alpha\beta} = \begin{pmatrix} p(1+N_1) & -\sigma \\ -\sigma & p(1-N_1) \end{pmatrix}, \tag{12}$$

where the signs are chosen so that shear stress and pressure are positive in our conventions. Although recent work has suggested that the stress tensor may be nonsymmetric in granular materials [52,99], we have observed that the stress tensor is symmetric for all of the flows we investigate here.

The granular temperature T is measured as

$$T = \sum_i v_i^2 - \left(\sum_i v_i\right)^2 + \frac{1}{2}\sum_i R_i^2\omega_i^2 - \frac{1}{2}\left(\sum_i R_i\omega_i\right)^2, \tag{13}$$

which is proportional to the kinetic temperature from Eq. (5), with the factor of 1/2 coming from the moment of inertia calculated for constant-density disks. The granular temperature is also proportional to the total energy in the system since there is no elastic energy in our hard-sphere simulations.

Last, for all of the numerical data that will be presented, we quantify the density of the system by its packing fraction ν. The packing fraction is defined as the area occupied by grains divided by the total area of the system. In our simulations, the packing fraction is proportional to both the mass density $\phi(\pi\phi=4\nu)$ and the number density $n(n\pi\langle R^2\rangle=\nu)$.

IV. TEST OF LOCAL RHEOLOGY

We first study the average relation between pressure p, shear stress σ, shear rate $\dot{\gamma}$, and granular temperature T in simple shear, using the periodic and translationally invariant LE cell. Next we compare these results with data obtained for the granular flow down an inclined plane.

A. Simple shear

1. Preliminary test

In all of the simple shear simulations presented here we have simulated 2500 grains in a square primitive cell, although we have conducted a limited number of simulations with up to 10 000 grains to ensure the accuracy of our observations. Because the contact dynamics algorithm induces some amount of numerical noise, the motion of a collection of grains driven at different shear rates is not expected to reproduce exactly the same phase-space trajectory. In Fig. 4 we show raw data of the normalized pressure $p\dot{\gamma}^{-2}$ as function of shear strain (strain rate multiplied by time), at a packing fraction of 0.8 with no friction and at two different values of the shear rate.

According to the invariance in Newton's equations $p\dot{\gamma}^{-2}$ should be independent of $\dot{\gamma}$, and this behavior is confirmed by the measurements in Fig. 4. Although the shear rates in the two plots differ by a factor of 10^4, the normalized pressure is virtually identical for both systems. Interestingly, not only do the steady-state values show no shear rate dependence, but the initial transient is virtually identical for both

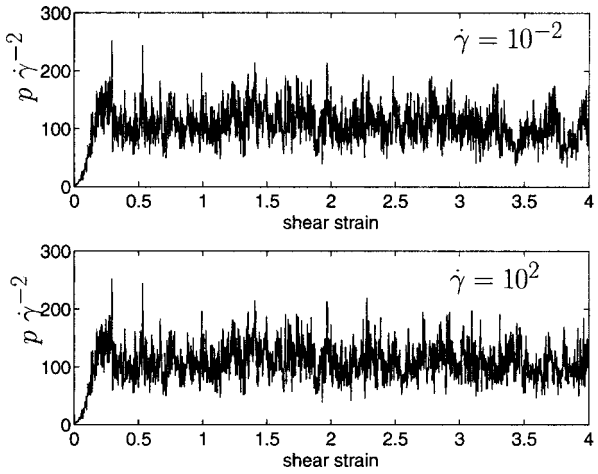

FIG. 4. Raw data of the pressure p (in arbitrary units) as a function of total shear for two frictionless granular materials with packing fraction 0.8. Data from simulations with different shear rates $\dot{\gamma}$ are shown. The top plot corresponds to $\dot{\gamma}=10^{-2}$ and the bottom to $\dot{\gamma}=10^2$. The pressure is normalized by $\dot{\gamma}^2$ which collapses the two data sets onto one master curve (i.e., with this rescaling the top and bottom traces appear essentially identical, up to numerical noise), as predicted by the invariance for hard-sphere systems.

values of $\dot{\gamma}$. The invariance in Newton's equations also predicts that $\sigma\dot{\gamma}^{-2}$ and $T\dot{\gamma}^{-2}$ are independent of $\dot{\gamma}$. For all of the simulations we have carried out these predictions from the invariance are upheld—although numerical noise often disrupts the perfect invariance for large values of shear strain, we see no change in the steady-state values of normalized pressure, shear stress, or granular temperature as the shear rate is varied at constant density. These results are not surprising—the contact dynamics algorithm is a method to simulate perfectly hard grains and the invariance in Newton's equations only holds for perfectly hard grains—but they offer assurance that the simulations are accurate.

The data in Fig. 4 also ensure us that the time step we use is small enough. From an algorithmic standpoint, scaling the strain rate amounts to a change in the time step. The good scaling of this data ensures that our algorithm solves the equations of hard spheres in a limit where the time step becomes irrelevant. It indicates that the number of contacts per grain in our simulation is not simply an artifact of the finite resolution of the contact dynamics methods.

For a granular material characterized by its pressure p, shear stress σ, temperature T, and strain rate $\dot{\gamma}$, we can construct three independent invariant and unitless quantities: σ/p, $\dot{\gamma}\langle R\rangle/\sqrt{T}$, and $mT/p\langle R\rangle^2$, where $\langle R\rangle$ and m are the average grain radius and mass. In Fig. 5 we show values of these three independent invariant quantities as a function of shear strain for a frictionless granular material at packing fraction of 0.8. For all quantities, steady flow is reached by a shear of approximately 0.5, and we will subsequently provide stationary data by time-averaging our measurements between strains of 2 and 10. The values of σ/p and $mT/p\langle R\rangle^2$ fluctuate much more than $\dot{\gamma}\langle R\rangle/\sqrt{T}$. This is due to the fact that σ and p depend on the forces between grains, which are highly fluctuating in the hard-sphere limit. In our simulations

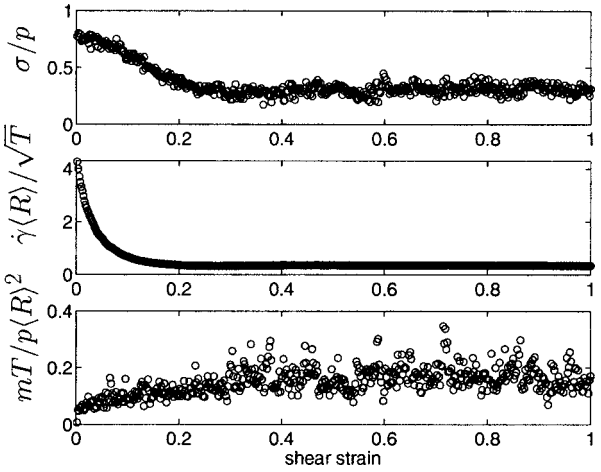

FIG. 5. Invariant and dimensionless quantities σ/p (top), $\dot{\gamma}\langle R\rangle/\sqrt{T}$ (middle), and $mT/p\langle R\rangle^2$ (bottom), where $\langle R\rangle$ is the average grain radius and m the average grain mass, as a function of shear strain for a frictionless granular material at packing fraction 0.8.

with 10 000 grains we observe that the fluctuations decrease while the average value remains constant. This suggests that in the limit of large system size, the fluctuations would disappear.

2. Liquid-solid transition

In Fig. 6 we present the steady-state values of $p\dot{\gamma}^{-2}/m$, $\sigma\dot{\gamma}^{-2}/m$, $T\dot{\gamma}^{-2}/\langle R\rangle^2$, and σ/p in simple shear for a range of high-packing-fraction systems that we have studied, at zero friction. Although there is relatively little change in these quantities for small packing fraction, for packing fractions larger that 0.75 there is a large increase in the values of the stresses and granular temperature. Additionally, the functional form of the stresses and granular temperature changes from approximately exponential to a function that grows faster than an exponential at $\nu \approx 0.75$.

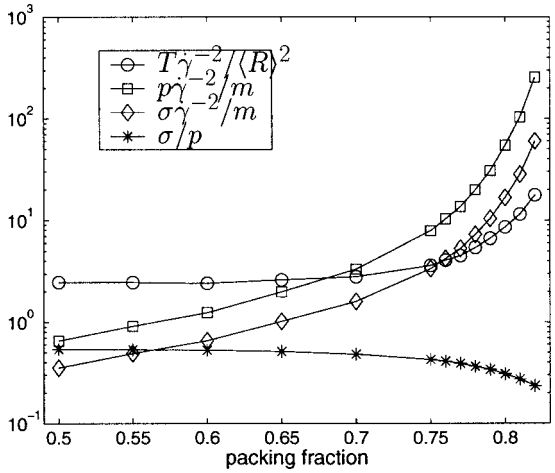

FIG. 6. Steady-state values of $p\dot{\gamma}^{-2}/m$ (squares), $\sigma\dot{\gamma}^{-2}/m$ (diamonds), $T\dot{\gamma}^{-2}/\langle R\rangle^2$ (circles), and σ/p (stars), where $\langle R\rangle$ is the average grain radius and m the average grain mass, as a function of packing fraction for a frictionless granular material.

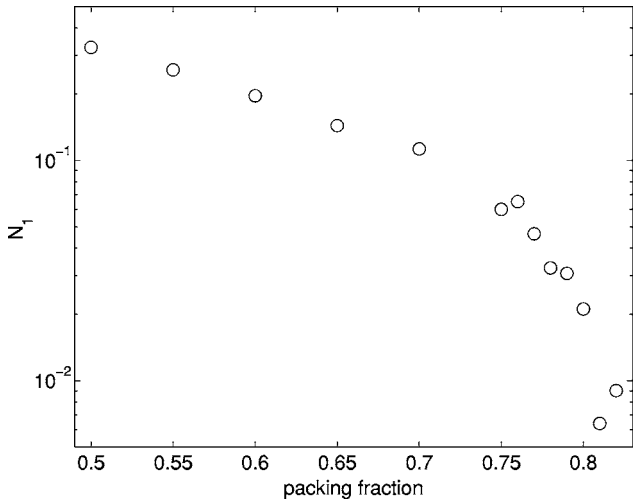

FIG. 7. First normal stress difference N_1 as a function of packing fraction for a frictionless granular material. $N_1 > 0$ for all packing fractions suggests that the granular materials are amorphous, and the decay of N_1 as a function of packing fraction suggests that nonkinetic effects dominate at high packing fraction.

Alam and Luding [100] have measured the steady-state values of the first normal stress difference N_1, defined via Eq. (12), in simple shear flow using a monodisperse collection of grains. In dilute flows, a nonvanishing value for N_1 results from collisional terms and the anisotropy in the distribution of velocities at Burnett order [101]. Alam and Luding reported that N_1 becomes negative at the onset of crystallization. We have thus measured the first normal stress difference in our system in order to ensure the absence of crystallization and as a signature of the breakdown of kinetic effects. The observation in Fig. 7 that $N_1 > 0$ for all packing fractions in our system is consistent with the observation that our system remains amorphous. The decay of N_1 over all packing fractions is consistent with the idea that kinetic effects become less important as the packing fraction increases, especially after $\nu \approx 0.75$ when N_1 begins to quickly decay.

In our numerical simulations, we expect the collisional contributions to the stress tensor to be negligible. A detailed study of the crossover between collisional and noncollisional regimes will be the topic of a future work [79]. For now we rely on the observation that the kinetic effects, as probed by the first normal stress difference, decay close to jamming. We also refer to prior works which support the same conclusion [76,77].

B. Flow down an inclined plane

In the simple shear cell the density and strain rate were specified, while stresses and granular temperature were measured. We now focus on flow down an inclined plane which provides a complementary situation. For incline flow, stresses are specified by the choice of an angle of inclination and by the gravitational field. Then the profiles of velocity and velocity fluctuations are measured and grant access to profiles of strain rate and granular temperature.

We report in Fig. 8 the packing fraction, average flow velocity, granular temperature, and $\dot{\gamma}\langle R\rangle/\sqrt{T}$ as a function of

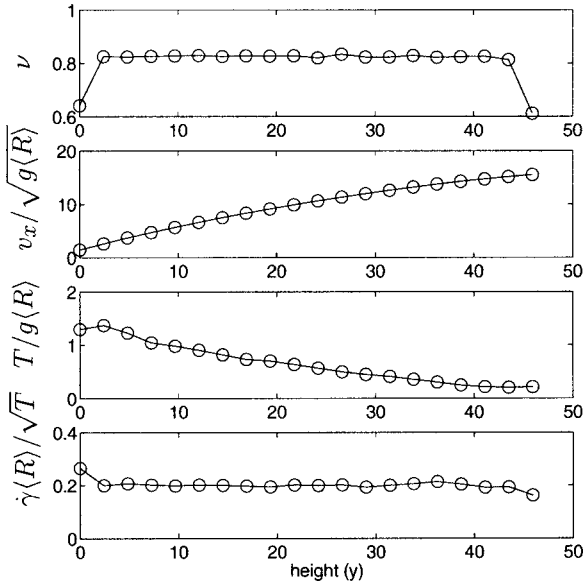

FIG. 8. Profiles of packing fraction, average velocity, granular temperature, and $\dot{\gamma}\langle R\rangle/\sqrt{T}$ as a function of the height (y) in the pile, measured in grain diameters, for a nonfrictional granular material at a 12° incline. The acceleration from gravity is denoted g, and the average grain radius is $\langle R\rangle$.

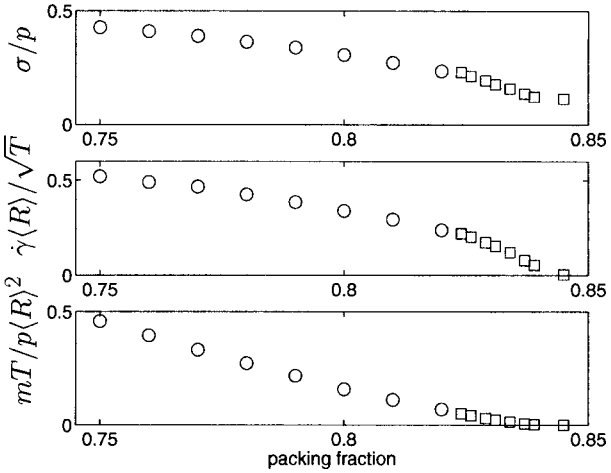

FIG. 9. The values of σ/p (top), $\dot{\gamma}\langle R\rangle/\sqrt{T}$ (middle), and $mT/p\langle R\rangle^2$ (bottom), where $\langle R\rangle$ is the average grain radius and m is the average grain mass, plotted as a function of packing fraction. Data from simple shear flow (circles) and flow down an incline (squares) match on the same curves. This suggests that there is a local rheology that is independent of the particular shearing geometry.

height for the steady flow of a nonfrictional granular material at an angle of 12°, with a total height of approximately 50 grains and a total of 2500 grains. Each point is determined by time-averaging the observable, in steady state, over an averaging height of about 3 grains. We have conducted simulations with heights and widths ranging between 25 and 100 grain diameters and have used different averaging techniques to ensure that our results do not depend on the size of the system or the averaging height.

We observe that, in the bulk central region of the flow, the packing fraction profile is uniform, the granular temperature is linear, and $\dot{\gamma}\langle R\rangle/\sqrt{T}$ is constant. The packing fraction decreases near $y=0$ because we have not included the stationary grains that make up the incline in this measure of packing fraction. When we include them, we see a slight increase in packing fraction near $y=0$. These observations hold in our simulations for all angles where the granular flow reaches a steady-state. We only use data from these steady-state flows in this paper. These observations are consistent with previous results by Silbert *et al.* [38,39].

There are four quantities of interest for incline flows—p, σ, $\dot{\gamma}$, and T—and these lead to three independent invariant quantities $\dot{\gamma}\langle R\rangle/\sqrt{T}$, σ/p, and $mT/p\langle R\rangle^2$. We observe in our simulations that all of these invariants are constant in the bulk of the incline flow. Therefore it is legitimate to compare these constant values with the constant values obtained from simple shear simulations. In Fig. 9 we present how the constant values of σ/p, $\dot{\gamma}\langle R\rangle/\sqrt{T}$, and $mT/p\langle R\rangle^2$ in the bulk of the flow depend on packing fraction and compare with our results from the simple shear cell. The fact that data from different shear flows fall on the same curves is remarkable and suggests that one theory should be able to describe simple shear and bulk incline granular flow.

Interestingly, the data from different flows do not overlap over a large interval of packing fraction: the flow down an inclined plane provides values at higher values of packing fraction than the simple shear cell. This is due to the fact that (i) steady flows down an incline plane are more easily reached for lower inclinations, hence higher densities, and (ii) the simple shear deformation is more difficult to integrate numerically at higher densities, because the periodic cell induces additional constraints that the contact dynamics algorithm manages with difficulty. Nevertheless, our use of two different configurations grants access to a broad range of $\dot{\gamma}\langle R\rangle/\sqrt{T}$, σ/p, and $mT/p\langle R\rangle^2$, and the sets of data are consistent with the existence of a unique, local relation between them as apparent in Fig. 9.

C. Origin of a local rheology

The excellent agreement between the two sets of data challenges the belief that nonlocal effects arise in dense granular flow. The data in Fig. 9 support a very conservative opinion: the motion of the grains decorrelates beyond some finite-length scale, in accordance with the fast decay of the pair correlation function (see Fig. 3).

In the bulk of the flow down an incline, it is possible to view layers of granular materials as effective simple shear cells. Such a layer of granular material at height y responds essentially as if it was confined in a simple shear cell, in the absence of body forces, with sustained external stresses $\sigma(y)$ and $p(y)$. Of course the invariance in Newton's equations, which holds exactly for the simple shear cell, is slightly broken by the gravitational force field. However, deep in the bulk of the flow, large confining stresses eventually dominate over the gravitational field. This approximate invariance suffices to predict that Bagnold's scaling must hold for the bulk regions of incline flows and explains the numerical data of Silbert and co-workers [38,39].

What is surprising is that the separation of microscopic and macroscopic scales is observable for the moderate

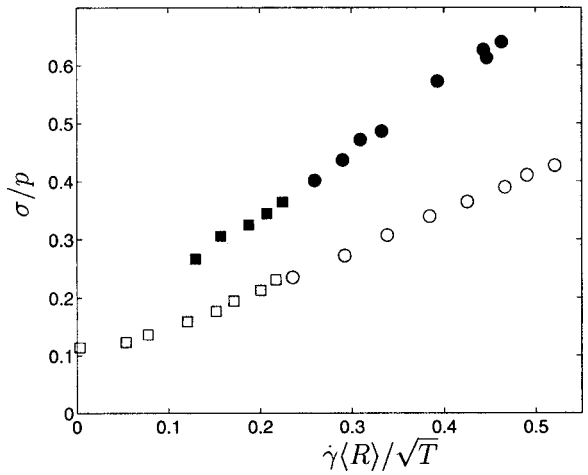

FIG. 10. σ/p plotted against $\dot{\gamma}\langle R\rangle/\sqrt{T}$ in steady-state simple shear flow (circles) and incline flow (squares). Solid symbols correspond to frictional granular materials with coefficient of friction $\mu=0.4$, and open symbols correspond to nonfrictional granular materials with $\mu=0$.

heights that we can access in our numerical simulations. This suggests that the length scale ℓ over which the motion of grains averages is smaller than the size of the grains themselves. This is consistent with the fact that, in a dense system, the region sampled by a given grain per strain unit is typically smaller than its size.

As we will see, our theory provides constitutive equations which relate the friction coefficient σ/p to the ratio $\dot{\gamma}\langle R\rangle/\sqrt{T}$. Anticipating the following sections, we present in Fig. 10 a plot of σ/p versus $\dot{\gamma}\langle R\rangle/\sqrt{T}$, with data from both the simple shear and incline flow geometries. As we will argue, such a plot is expected to be the granular counterpart of a stress versus strain rate plot for a glassy material [69], with the shear stress normalized by the pressure and the strain rate normalized by the granular temperature. We see here that the analogy is striking: when rescaled properly the granular material presents typical features of normal yield stress fluids [102]. For large values of normalized strain rate, the normalized stress is proportional to the normalized strain rate. For small values of the normalized strain rate, the linear relationship no longer holds and there is a yield (normalized) stress at zero (normalized) strain rate.

V. CONSTITUTIVE EQUATIONS

Several interesting results stem from the preceding observations: (i) for a given density, only invariant quantities are relevant to describe the state of a granular flow; (ii) when invariant quantities are considered, the granular material displays a "normal" rheology of a yield stress liquid; and (iii) the rheology measured in the Lees-Edward cell extrapolates to the rheology measured from bulk data of incline flow.

These observations foster our hope to construct local constitutive equations for dense granular materials. For sure, we will not attempt here to produce "local" constitutive equations in the sense used in kinetic theory studies of dilute granular flows [85]. Instead, we wish to present an elementary model of granular flow in the spirit of thermodynamic models of material deformation in amorphous solids. Recent advances have been made in this field, with the introduction by Falk and Langer of STZ theory [70,71]. This theory constructs a "hydrodynamic" description of material deformation through the introduction of a small number of state variables and the prescription for their evolution in time. Although these "rate-and-state" models are clearly limited by their typically phenomenological constructions, they are motivated by plausible microscopic mechanisms and explore the corresponding consequences through comparisons with experimental data [103]. Before addressing the specificities of the STZ formulation of constitutive equations, we wish to argue that the scaling invariance of Newton's equations calls for a parallel scaling form of the constitutive equations.

A. Scaling form for constitutive equations

In general, constitutive equations should provide a relation between the stresses and strain rate and a set of state variables $\{\psi_i\}$ which characterize the internal structure of the granular material. For granular materials the granular temperature T plays a quite specific role as a state variable. Other state variables are expected to account only for geometric properties of the granular packing.

1. Conservation of energy

Ogawa [104] was the first to recognize that in granular materials the temperature cannot be prescribed by a thermal bath, but is set by energy balance. Kinetic theory provides estimates for the energy dissipation rate in dilute systems, hence providing approximations for the equation of motion which governs granular temperature. As a result, the notion of granular temperature has been tied to kinetic theory.

Granular temperature, however, is not reserved for the description of dilute flows. It is relevant in all inertial flows since, as discussed previously, there is no quasistatic limit for hard spheres, even infinitely close to jamming. In particular the dense flows of our simulations do not verify the assumptions of kinetic theory, yet in these inertial regimes kinetic energy is a perfectly relevant physical observable and is set by energy balance.

At any time, the variation of kinetic energy results from the balance between external work done on the system and dissipative mechanisms. Because the system explores phase-space trajectories at a velocity proportional to $\sqrt{T}$, the rate of energy dissipation should scale as $\sqrt{T}T$. The square root gives the frequency of dissipative events, and each event dissipates an energy proportional to T. Energy is introduced to the system via the external forcing with a rate of $\sigma\dot{\gamma}$. Therefore, the energy balance equation should be of the form

$$\phi\dot{T} = \sigma\dot{\gamma} - \alpha(\phi,\{\psi_i\})\phi T\frac{\sqrt{T}}{\langle R\rangle}, \tag{14}$$

where ϕ represents the mass density. The factor α is a unitless geometric factor which depends on the relative positions of grains, but should not incorporate any further dependence on T or the stress tensor. In particular, it should depend on

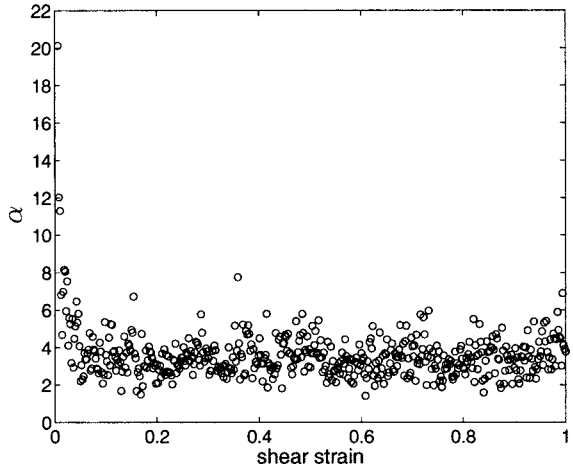

FIG. 11. α from Eq. (14) as a function of shear strain for a simple shear flow of a nonfrictional granular material at packing fraction 0.8. For small values of shear α varies slightly, but quickly becomes constant at a shear strain of approximately 0.04.

the mass density ϕ and possibly on other state variables $\{\psi_i\}$ which characterize the geometrical structure of the granular packing. By scaling invariance, the steady-state value of α should depend of ϕ only.

This equation has a similar form to the energy conservation equation derived in kinetic theory [105]. This is no surprise since kinetic theory must uphold the invariance of Newton's equations. Kinetic theory provides an estimate for $\alpha(\phi)$, and it is possible that even in dense flows this estimate remains reasonable for nonfrictional grains. However, multibody collisions may induce departure of this relation from the predictions of kinetic theory.

In Fig. 11 we present a plot of α as a function of shear strain for a nonfrictional granular material in simple shear flow, calculated via Eq. (14). We observe a dynamic in α at the start of the simulation which quickly disappears. The dynamic is likely due to the effects of an unknown state variable ψ_i.

2. Constitutive relation

Since granular temperature is defined as the frequency of elementary events along phase-space trajectories, the strain rate should scale as

$$\frac{\dot{\gamma}\langle R\rangle}{\sqrt{T}} = f\left(\frac{\sigma}{p}, \frac{mT}{p\langle R\rangle^2}, \{\psi_i\}\right), \tag{15}$$

where f denotes an unknown function and, once again, the state variables $\{\psi_i\}$ are purely geometric.

If we combine Eq. (15) with Eq. (14) in steady state where $\dot{T}=0$, then we see that

$$\sigma = \left[\alpha\phi\langle R\rangle^2 F\left(\frac{\sigma}{p}, \psi_i\right)^{-3}\right]\dot{\gamma}^2, \tag{16}$$

where F is equal to the function f, with $mT/p\langle R\rangle^2$ evaluated using Eq. (14). This equation implies that if constitutive relations are written in the form of Eqs. (14) and (15), then Bagnold's scaling is upheld.

In the rest of this section we study the STZ formulation of constitutive equations and apply it to dense granular materials. We will see that the STZ theory, when applied to granular materials, makes a prediction for the function f in Eq. (15).

B. STZ theory

1. Basics

The shear transformation zone theory of amorphous solids was proposed in [70,71,103,106–108] as a mean-field model to account for the behavior of dense amorphous materials at low temperature. The theory is motivated by observations from simulations [109–113] and experiments [114] which suggest that plastic deformation in amorphous materials results from nonaffine rearrangements of small clusters of particles [115]. Additionally, Falk and Langer were able to show that there exist different types of zones which present a preferential response to different orientations of shear forces. They introduced the densities of these zones as state variables to characterize the internal structure of the molecular packing.

Central to the theory is the assumption that once an STZ undergoes an elementary rearrangement in a given direction it is unlikely that it can shear again in the same direction, although it can easily shear in the reverse direction. Thus zones appear as two-state systems, the states corresponding to the zone orientation being aligned (denoted "−") or antialigned (denoted "+") with the shear stress. A rearrangement corresponds to a transition of a zone from a $\pm$ state into a $\mp$ state and vice versa. The plastic shear rate is given by the rate at which STZ's respond to external stresses:

$$\dot{\gamma} \propto R_+ n_+ - R_- n_-, \tag{17}$$

where $R_\pm$ are the stress-dependent probabilities that zones of $\pm$ types are transformed into one another.

This constitutive relation must be complemented with an equation of motion for the densities $n_\pm$, which is postulated to be of the form

$$\dot{n}_\pm = R_\mp n_\mp - R_\pm n_\pm + w(\xi - \zeta n_\pm). \tag{18}$$

The first two terms correspond to the transformation of STZ's into their two possible states. The last term accounts for the fact that STZ's are renewed by the overall macroscopic deformation: it contains a creation and destruction rate, both proportional to the plastic work w of external forces per time unit.

2. Observation of directional response

Before applying STZ theory to granular materials, we check that the same qualitative observations as in [70] can be performed in these systems—namely, that nonaffine motion occurs in localized regions and that the positions of the localized regions depend sensitively on the orientation of the shear. The first observation motivates the choice of density of STZ's as a state variable, and the second observation shows that each STZ has an orientation and therefore only responds to a certain orientation of shear stress.

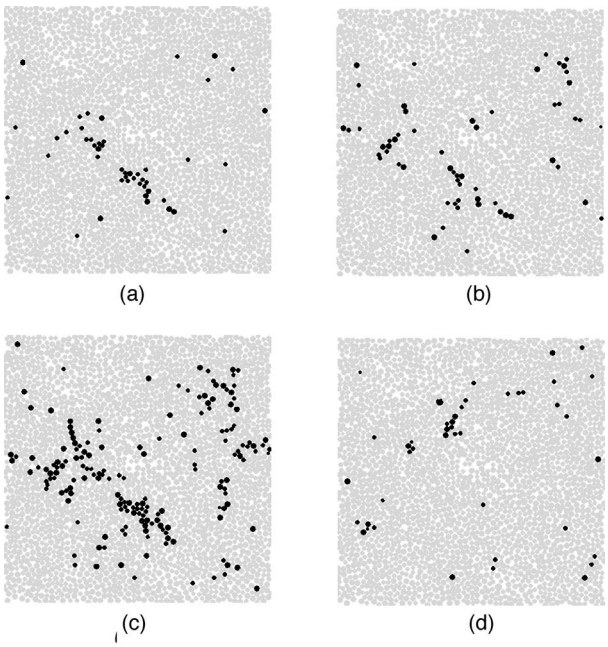

FIG. 12. Screenshots of granular materials in steady-state simple shear flow with grains undergoing nonaffine displacement, colored black. In (a) the system is sheared from 0 to 0.05, in (b) the system is sheared from 0.1 to 0.15, in (c) the system is sheared from 0 to 0.15, and in (d) the system is sheared in the opposite direction, from 0 to −0.05.

These observations are based on a measure of the nonaffinity of the deformation of a cluster of a few molecules or grains. Following [70], the grains undergoing a nonaffine rearrangement can be determined by calculating, for each grain, the local strain rate at time $t-\Delta t$. Then, by measuring the difference D between the actual position at a later time t and the position predicted from the local strain rate at time $t-\Delta t$, we can determine which grains have moved nonaffinely in the time period Δt. In practice, D is determined by minimizing

$$\tilde{D}^2(t,\Delta t) = \sum_n \sum_i \left(r_n^i(t) - r_0^i(t) - \sum_j (\delta_{ij} + \dot{\gamma}_{ij}) \times [r_n^j(t-\Delta t) - r_0^j(t-\Delta t)] \right)^2, \tag{19}$$

with respect to the shear rate $\dot{\gamma}_{ij}$, where the indices i and j are spatial coordinates and the index n runs over all grains within two diameters of the reference grain, labeled by the index $n=0$. The minimum value of $\tilde{D}$, denoted D, is an approximation of the local deviation from affine displacement for the reference grain in the time interval $[t-\Delta t, t]$. If there is no nonaffine motion, then the motion of each individual grain should be completely determined by a local shear rate and $D=0$. If there is nonaffine motion, then $D>0$.

We have applied this test for nonaffine motion to granular materials in simple shear to produce Fig. 12. This figure is the counterpart of Fig. 3 in [106] and Fig. 7 in [70], which were created from simulations of an amorphous Lennard-Jones solid. Each picture has been created by shearing an identical initial arrangement of particles in a certain direction. D is the local measure of the nonaffinity obtained by comparison between the initial and final states. If D is larger than a reference value, the particle is said to have moved nonaffinely and is colored black.

In Fig. 12(a) the system is sheared from strains of 0–0.05 and in Fig. 12(b) the system is sheared to from strains of 0.1–0.15. We notice that there is a tendency for the regions of nonaffine displacement to form clusters, and the size of the resulting nonaffine regions is about the same in both (a) and (b). In (c) the system is sheared from strains of 0–0.15 and now the size of the nonaffine regions increases, suggesting many more fundamental rearrangements of STZ's in the larger time period. In (d) the system is sheared from strains of from 0 to −0.05 (in the *opposite* direction), starting from the same initial configuration as in (a). Once again we observe that the nonaffine regions tend to form clusters. However, in comparing (a) and (d), we notice that the size of the nonaffine regions is about the same in the two figures, but the locations are different. If the regions undergoing nonaffine displacement did not have an orientation, we would expect nonaffine motion to occur in the same location, regardless of the orientation of the stress. However, this is not the case and the data in Fig. 12 suggest that the regions that move nonaffinely have an orientation. This is qualitative evidence that the core assumptions of STZ theory are upheld in granular materials.

3. STZ theory for granular materials

The STZ densities $n_\pm$ account for structural properties of a molecular or granular packing. They are thus expected to depend on the positions of grains, orientations and distribution of forces, and orientations of velocities, but not on the overall amplitude of the forces or amplitude of velocities. Following [69], these functions are determined using the invariance in Newton's equations. Since w is equal to the plastic work done on the system per unit time, it should be proportional to $\sigma\dot{\gamma}$. In order to make w invariant, we normalize by pressure so that $w=\sigma\dot{\gamma}/p$. As for $R_\pm$, because of the invariance in Newton's equations, we can separate the rate at which an STZ attempts to rearrange from the probability that an attempt leads to a successful rearrangement. The attempt rate must be proportional to $\sqrt{T}$ which sets the microscopic event rate, and the probability to rearrange is written as an exponential activation factor of the invariant form $e^{\pm\kappa\sigma/p}$. This yields $R_\pm \propto \sqrt{T}e^{\pm\kappa\sigma/p}$.

Combining the expressions for $R_\pm$ and w with Eqs. (17) and (18), while making a change of variables from $n_\pm$ to $\Delta \propto n_- - n_+$ and $\Lambda \propto n_- + n_+$, yields the following STZ equations for granular materials:

$$\dot{\gamma} \propto \sqrt{T}[\Lambda \sinh(\kappa\sigma/p) - \Delta \cosh(\kappa\sigma/p)],$$

$$\dot{\Delta} \propto \dot{\gamma}\left(1 - \zeta\frac{\sigma}{p}\Delta\right),$$

$$\dot{\Lambda} \propto \dot{\gamma}\frac{\sigma}{p}(1-\Lambda). \tag{20}$$

Λ denotes the total density of zones, and Δ measures the mismatch between zones, of different orientations and therefore is related to the anisotropy of the granular packing. κ and ζ are constants that do not depend on the macroscopic variables $\dot{\gamma}$, T, σ, or p. However, we would expect these constants to depend on properties of the grains such as shape, distributions of radii, restitution coefficients, friction coefficients, or other local static variables, including density.

These equations determine the shear rate of the flow through the state variables Δ and Λ, which encode the microscopic structure of the material. Let us note that other recent theories of dense granular flows introduce state variables of a rather different nature to account for jamming. For example, Aranson and co-worker consider that relevant state variables are associated with the numbers of solidlike contacts between grains [64–66]. Bazant introduces a density of "spots" of free volume, [67,68] which are closely related to some of our works on free-volume dynamics in dense materials [116–119]. These models rely on state variables which are intrinsically scalar. The specificity of the STZ equations is that the quantity Δ is "homogeneous" to a tensor as it is related to the anisotropy of the contact network.

4. Steady states

The STZ equations present two types of steady-state solutions [69–71]. One branch of solutions represents a jammed state $\dot{\gamma}=0$ and occurs when $\Delta/\Lambda=\tanh(\kappa\sigma/p)$. The other branch of solution represents the steady flow and occurs when $\Lambda=1$ and $\Delta=p/(\zeta\sigma)$.

An elementary analysis of the phase diagram of this dynamical system indicates that the jammed state is stable if and only if

$$\zeta\frac{\sigma}{p}\tanh\left(\kappa\frac{\sigma}{p}\right) \leqslant 1 \tag{21}$$

and the flowing state is stable otherwise. The limit of stability occurs at a critical angle θ^*, which is the solution of

$$\zeta \tan\theta^* \tanh(\kappa \tan\theta^*) = 1. \tag{22}$$

θ^* is identified as the repose angle of our granular material.

In the steady flowing regime $\dot{\gamma}\geqslant 0$ and STZ theory yields the constitutive relation:

$$\frac{\dot{\gamma}\langle R\rangle}{\sqrt{T}} \propto \left(\sinh(\kappa\sigma/p) - \frac{p}{\sigma\zeta}\cosh(\kappa\sigma/p)\right), \tag{23}$$

where we have inserted a factor of the average grain radius $\langle R\rangle$ to match units. In particular, in the limit when the ratio $\dot{\gamma}\langle R\rangle/\sqrt{T}$ vanishes, σ/p converges towards $\tan\theta^*$. Therefore the STZ theory accommodates cases where there is a residual pressure and shear stress at zero shear rate and predicts that in this case the shear stress will be proportional to the pressure.

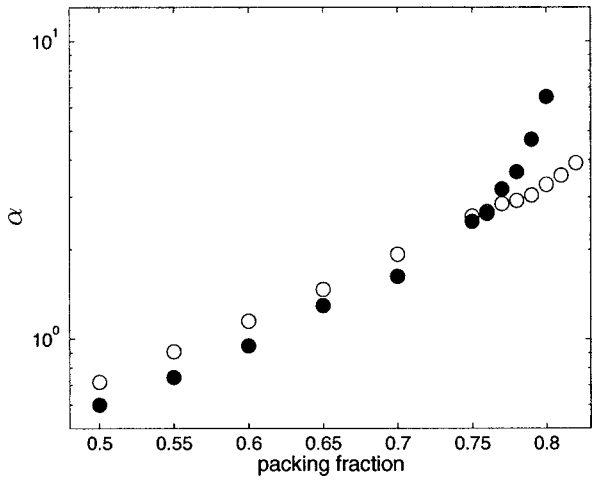

FIG. 13. Density dependence of α, defined through Eq. (14), for frictional (solid symbols) and nonfrictional (open symbols) simple shear flows.

C. Numerical tests

The constitutive equations for granular materials introduced in this paper are entirely specified by Eqs. (14) and (20). We now compare the steady-state relations predicted by these equations with our numerical data, which provides independent access to σ, p, T, and $\dot{\gamma}$ in different shearing geometries.

We first test Eq. (14) in simple shear flow. We find that for all densities investigated, much like Fig. 11, α is constant as a function of shear strain. Additionally we find that the steady-state value only depends on the density and friction coefficient. We present the measured steady-state values of α in Fig. 13 as a function of packing fraction, for frictionless ($\mu=0$) and frictional ($\mu=0.4$) granular materials. For frictionless granular materials α appears to vary exponentially as a function of packing fraction, whereas for frictional granular materials α does not take on an obvious functional form.

Next, we test the steady-state STZ prediction from Eq. (23). In Fig. 14 we have plotted numerical data of σ/p as a function of $\dot{\gamma}\langle R\rangle/\sqrt{T}$ for frictional and nonfrictional granular materials in both simple shear flow and incline flow. The line drawn through the data is a fit to Eq. (23). The fit matches the data from both flowing geometries very well.

To construct the fit, we have used the data from *the simple shear cell only*. This fit permits us to extrapolate the rheology for the flow down an incline plane, even at the approach of the repose angle. This demonstrates that an accurate determination of the coefficients from the STZ equation (23) in one shearing geometry allows for a prediction in a different shearing geometry.

VI. CONCLUSION

We have implemented numerical simulations of dense granular flows in order to clarify the microscopic origin of jamming and the specific assumptions needed to construct the STZ formulation of constitutive equations for dense granular flows.

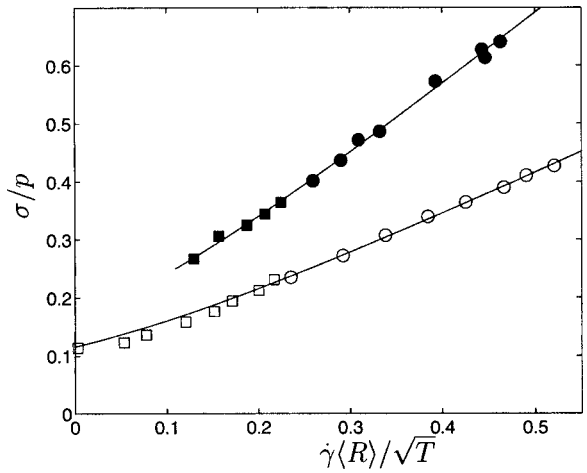

FIG. 14. σ/p plotted against $\dot{\gamma}\langle R\rangle/\sqrt{T}$ for frictional (solid symbols) and nonfrictional (open symbols) granular materials. The circles correspond to data from simple shear flow and the squares to data from steady-state incline flow. The line is a best fit to the steady-state STZ prediction from Eq. (23), where only the data from the simple shear flow geometry were used to construct the best fit. This shows that STZ theory properly predicts the outcome of incline flow experiments once the parameters (which depend only on grain properties) are determined from simple shear experiments.

Our first goal was to obtain detailed information on dense granular flows, in particular on the locality of the constitutive relation. For this purpose we implemented two different simulation configurations: a simple shear cell, with Lees-Edwards periodic boundary conditions and Sllod equations of motion, and the flow of a granular material down a rough incline. In both configurations we measured the components of the stress tensor, packing fraction, strain rate, and granular temperature.

We have also observed the normal stress difference and shown that it vanishes in dense flows so that, in this regime, shear stress and pressure completely characterize the stress tensor. In each configuration we studied, the rheology of dense granular materials is entirely specified by five quantities: shear stress σ, pressure p, packing fraction ν, strain rate $\dot{\gamma}$, and granular temperature T. In the shear cell ν and $\dot{\gamma}$ are prescribed, and in the flow down an incline σ and p are prescribed. The rheology of the granular material requires us to specify three relations which determine the remaining unknowns. There are many equivalent ways these relations can be formulated, but we wished to formulate them in a way that emphasized the invariance of Newton's equations and the expected scaling form of constitutive equations.

We found, as anticipated in [69], that the relation between quantities $\dot{\gamma}\langle R\rangle/\sqrt{T}$ and σ/p is remarkably similar to the stress-strain rate relation in a normal elastoplastic transition. We were surprised to observe the quality of the fit to the data of Fig. 14 with expression (23) without any density dependence of the parameters of the theory. We would have expected that these parameters might involve a strong density dependence. This observation strengthens the hypothesis that the distinguishing feature of granular materials is the way energy balance is prescribed and otherwise, once the variables are appropriately rescaled, they behave like "normal" materials.

Another relation emerges naturally from the expectation that energy balance in granular materials should take the form as in Eq. (14). The density-dependent parameter α accounts for the rate of dissipation of energy, and we would expect it to be reasonably captured by collisional integrals of the type used in kinetic theory (at least for nonfrictional materials). A proper derivation of energy dissipation in dense flows now appears as an accessible yet challenging issue that we wish to examine in future works.

Finally, a third relation remains to be specified. This relation can be, for example, a prescription for σ/p or $\dot{\gamma}\langle R\rangle/\sqrt{T}$ as a function of packing fraction. We observed this relation in Fig. 9, but did not attempt to model it. Other works of ours [116–119], as well as Bazant's "spot" model [67,68], attempt to account for the role of free-volume fluctuations in the rheology of dense materials. A related idea is the introduction by Aranson *et al.* [64–66] of a state variable associated with the density of solidlike contacts. These approaches focus more directly on the density dependence of the response of dense granular materials and may thus provide the missing relation.

As we see, the STZ theory correctly predicts one among three relations which are necessary for a complete description of dense granular flows. This relation, coupled to Bagnold's scaling, suffices to account for the shape of the velocity profile down an incline. However, it does not account for the overall amplitude of the velocity profile or the uniform value of the density as a function of $\tan\theta$.

Note that we have compared here data from a Lees-Edward cell with the rheology of a flow down an inclined plane in the limit where the height of the granular material is large. The agreement between the two sets of data indicates that there is no long-range structure which governs the flow. This does not mean, however, that no gradient or diffusive terms should ever appear in the final form of the rheology of granular flows. In particular, we expect that a diffusive term should arise in Eq. (14), but in the large-height limit this diffusive term does not appear in the bulk rheology.

This brings us to the observations by Pouliquen [84] of a relation $h_{\mathrm{stop}}(\theta)$ which governs jamming. These observations have led to the idea that nonlocal constitutive equations might be required to capture the rheology of granular materials. However, we expect these observations to be "normal" finite-size effects. For example, it was observed in [69] that an exponentially decaying kernel in place of w in Eq. (18) was sufficient to account for large values of $h_{\mathrm{stop}}(\theta)$ when $\theta\rightarrow\theta^{*}$. The analytical form of the kernel used in this work was consistent with an exponential decay of correlation in the system, again consistent with the notion that short-range correlations suffice to understand these effects. But other theories also successfully introduce finite length scales to account for macroscopic phenomena. In particular, the "spot" model [67,68] relates such a length scale to the size of diffusive regions of high free volume, which seems rather complementary to our viewpoint. It seems that the existence of a finite size for rearranging zones suffices to account for the emergence of large length scales close to jamming.

Another puzzling observation by Pouliquen was that the

amplitude of the velocity profile seemed to scale as $1/h_{\mathrm{stop}}(\theta)$. As we saw previously, this amplitude is governed by $\alpha(\nu)$ and a missing relation between, e.g., σ/p and ν. We thus cannot provide an interpretation for these observations.

Our observations on a model system strongly suggest that the definition of a local rheology for granular materials is, in principle, possible. Moreover, we see emerging from our analysis some state variables and their equations of motion. This now opens a very exciting route toward a set of local hydrodynamic equations for dense granular materials: such equations will offer a predictive tool to further address fundamental and practical questions in numerous situations where flow equations for granular materials are much needed.

ACKNOWLEDGMENTS

This work was supported by the William M. Keck Foundation, the MRSEC program of the NSF under Award No. DMR00-80034, the James S. McDonnell Foundation, NSF Grant No. DMR-9813752, the Lucile Packard Foundation, the Mitsubishi Corporation, and the National Science Foundation under Grant No. PHY99-07949.

[1] A. Schofield and C. P. Wroth, *Critical State in Soil Mechanics* (McGraw-Hill, New York, 1968).
[2] R. L. Brown and J. C. Richard, *Principles of Powder Mechanics* (Pergamon, New York, 1970).
[3] K. H. Roscoe, Geotechnique **20**, 129 (1970).
[4] R. M. Nedderman, *Statics and Kinematics of Granular Materials* (Cambridge University Press, Cambridge, England, 1992).
[5] H. M. Jaeger and S. R. Nagel, Science **255**, 1523 (1992).
[6] A. Mehta and G. C. Barker, Rep. Prog. Phys. **57**, 383 (1994).
[7] H. M. Jaeger and S. R. Nagel, Rev. Mod. Phys. **68**, 1259 (1996).
[8] H. M. Jaeger, S. R. Nagel, and R. P. Behringer, Rev. Mod. Phys. **68**, 1259 (1996).
[9] Jacques Duran, *Sables, Poudres et Grains* (Éditions Eyrolles, Paris, 1997).
[10] P. G. de Gennes, Physica A **261**, 267 (1998).
[11] J. Rajchenbach, Adv. Phys. **49**, 229 (2000).
[12] L. P. Kadanoff, Rev. Mod. Phys. **71**, 435 (1999).
[13] S. F. Edwards and D. V. Grinev, Adv. Phys. **51**, 1669 (2002).
[14] J. M. Hill and Y. H. Wu, Proc. R. Soc. London, Ser. A **438**, 67 (1992).
[15] D. Harris, Proc. R. Soc. London, Ser. A **450**, 37 (1995).
[16] J. M. Hill and X. M. Zheng, Acta Polytech. Scand., Mech. Eng. Ser. **118**, 97 (1996).
[17] S. B. Savage, J. Fluid Mech. **92**, 53 (1979).
[18] S. B. Savage and D. J. Jeffrey, J. Fluid Mech. **110**, 255 (1981).
[19] J. T. Jenkins and S. B. Savage, J. Fluid Mech. **130**, 187 (1983).
[20] C. K. K. Lun, S. B. Savage, D. J. Jeffrey, and N. Chepurniy, J. Fluid Mech. **140**, 223 (1984).
[21] J. T. Jenkins and M. W. Richman, Phys. Fluids **28**, 3485 (1985).
[22] C. K. K. Lun and S. B. Savage, J. Appl. Mech. **54**, 47 (1987).
[23] S. B. Savage, in *Theoretical and Applied Mechanics*, edited by P. Germain, M. Piau, and D. Caillerie (Elsevier, Amsterdam, 1989), pp. 241–266.
[24] C. S. Campbell, Annu. Rev. Fluid Mech. **22**, 57 (1990).
[25] K. Hutter and K. R. Rajagopal, Continuum Mech. Thermodyn. **6**, 81 (1994).
[26] N. Sela and I. Goldhirsch, Phys. Fluids **7**, 507 (1995).
[27] N. Sela, I. Goldhirsch, and S. H. Noskowicz, Phys. Fluids **8**, 2337 (1996).
[28] N. Sela and I. Goldhirsch, J. Fluid Mech. **361**, 41 (1998).
[29] J. W. Dufty, Adv. Complex Syst. **4**, 397 (2001).
[30] H. Hertz, J. Reine Angew. Math. **92**, 156 (1881).
[31] K. L. Johnson, *Contact Mechanics* (Cambridge University Press, Cambridge, England, 1985).
[32] E. Azanza, Ph.D. thesis, École Nationale des Ponts et Chausées, 1998.
[33] E. Azanza, F. Chevoir, and P. Moucheront, J. Fluid Mech. **400**, 199 (1999).
[34] N. Mitarai and H. Nakanishi, Phys. Rev. Lett. **94**, 128001 (2005).
[35] R. A. Bagnold, Proc. R. Soc. London, Ser. A **255**, 49 (1954).
[36] R. A. Bagnold, Proc. R. Soc. London, Ser. A **295**, 219 (1966).
[37] M. L. Hunt, R. Zenit, C. S. Campbell, and C. E. Brennen, J. Fluid Mech. **452**, 1 (2002).
[38] L. E. Silbert, D. Entas, G. S. Grest, T. C. Halsey, D. Levine, and S. J. Plimpton, Phys. Rev. E **64**, 051302 (2001).
[39] L. E. Silbert, J. W. Landry, and G. S. Grest, Phys. Fluids **15**, 1 (2003).
[40] J. Rajchenbach, Eur. Phys. J. E **14**, 367 (2004).
[41] P. Mills, D. Loggia, and M. Tixier, Europhys. Lett. **45**, 733 (1999).
[42] P. Mills, M. Tixier, and D. Loggia, Eur. Phys. J. E **1**, 5 (2000).
[43] F. Chevoir, M. Prochnow, J. Jenkins and P. Mills (unpublished).
[44] D. Ertaş and T. C. Hasley, Europhys. Lett. **60**, 931 (2002).
[45] GDR MIDI, Eur. Phys. J. E **14**, 341 (2004).
[46] P. A. Cundall and O. D. L. Strack, Geotechnique **29**, 47 (1979).
[47] A. Drescher and G. Dejossel, J. Mech. Phys. Solids **20**, 337 (1972).
[48] D. M. Mueth, H. M. Jaeger, and S. R. Nagel, Phys. Rev. E **57**, 3164 (1998).
[49] D. W. Howell, R. P. Behringer, and C. T. Veje, Chaos **9**, 559 (1999).
[50] D. Howell, R. P. Behringer, and C. Veje, Phys. Rev. Lett. **82**, 5241 (1999).
[51] K. I. Kanatani, Int. J. Eng. Sci. **17**, 419 (1979).
[52] N. Mitarai, H. Hayakawa, and H. Nakanishi, Phys. Rev. Lett. **88**, 174301 (2002).
[53] S. B. Savage, J. Fluid Mech. **377**, 1 (1998).
[54] W. Losert, L. Bocquet, T. C. Lubensky, and J. P. Gollub, Phys. Rev. Lett. **85**, 1428 (2000).

[55] L. Bocquet, J. Errami, and T. C. Lubensky, Phys. Rev. Lett. **89**, 184301 (2002).
[56] L. Bocquet, W. Losert, D. Schalk, T. C. Lubensky, and J. P. Gollub, Phys. Rev. E **65**, 011307 (2001).
[57] S. B. Savage, in *Mechanics of Granular Materials: New Models and Constitutive Relations*, edited by J. T. Jenkins and M. Satake (Elsevier, Amsterdam, 1983), pp. 261–282.
[58] P. C. Johnson and R. Jackson, J. Fluid Mech. **176**, 67 (1987).
[59] P. C. Johnson, P. Nott, and R. Jackson, J. Fluid Mech. **210**, 501 (1990).
[60] J. T. Jenkins and E. Askari, J. Fluid Mech. **223**, 497 (1991).
[61] K. G. Anderson and R. Jackson, J. Fluid Mech. **41**, 145 (1992).
[62] M. Y. Louge, Phys. Rev. E **67**, 061303 (2003).
[63] O. Pouliquen and R. Gutfraind, Phys. Rev. E **53**, 552 (1996).
[64] I. S. Aranson, L. S. Tsimring, and V. M. Vinokur, Phys. Rev. E **60**, 1975 (1999).
[65] I. S. Aranson and L. S. Tsimring, Phys. Rev. E **64**, 020301(R) (2001).
[66] D. Volfson, L. S. Tsimring, and I. S. Aranson, Phys. Rev. E **68**, 021301 (2003).
[67] Martin Z. Bazant, e-print cond-mat/0307379.
[68] Martin Z. Bazant, e-print cond-mat/0501130.
[69] A. Lemaître, Phys. Rev. Lett. **89**, 064303 (2002).
[70] M. L. Falk and J. S. Langer, Phys. Rev. E **57**, 7192 (1998).
[71] M. L. Falk and J. S. Langer, MRS Bull. **25**, 40 (2000).
[72] C. S. Campbell, J. Fluid Mech. **465**, 261 (2002).
[73] Y. Zhang and C. S. Campbell, J. Fluid Mech. **237**, 541 (1992).
[74] C. S. Campbell, in *Powders and Grains 93*, edited by C. Thornton (A. A. Balkema, Rotterdam, 1993), pp. 289–294.
[75] V. V. R. Natarajan, M. L. Hunt, and E. D. Taylor, J. Fluid Mech. **304**, 1 (1995).
[76] C. S. Campbell, P. W. Cleary, and M. Hopkins, J. Geophys. Res. **100**, 8267 (1995).
[77] A. V. Potapov and C. S. Campbell, Phys. Fluids **8**, 2884 (1996).
[78] J. Choi, A. Kudrolli, R. R. Rosales, and M. Z. Bazant, Phys. Rev. Lett. **92**, 174301 (2004).
[79] G. Lois, A. Lemaître, and J. M. Carlson, e-print cond-mat/0507286.
[80] X. Jia, C. Caroli, and B. Velicky, Phys. Rev. Lett. **82**, 1863 (1999).
[81] H. A. Makse, N. Gland, D. L. Johnson, and L. Schwartz (unpublished).
[82] C. S. Campbell and C. E. Brennen, J. Fluid Mech. **151**, 167 (1985).
[83] H. J. Herrmann and S. Luding, Continuum Mech. Thermodyn. **10**, 189 (1998).
[84] O. Pouliquen, Phys. Fluids **11**, 542 (1999).
[85] I. Goldhirsch, Annu. Rev. Fluid Mech. **35**, 267 (2003).
[86] C. S. O'Hern, L. E. Silbert, A. J. Liu, and S. R. Nagel, Phys. Rev. E **68**, 011306 (2003).
[87] F. Chevoir *et al.*, in *Powders and Grains*, edited by Y. Kishino (Swets and Zeitliger, Lisse, The Netherlands, 2001), pp. 399–402.
[88] J. J. Moreau, in *Nonsmooth Mechanics and Application: Courses and Lectures*, edited by J. J. Moreau and P. D. Panagiotopoulos (Springer-Verlag, Vienna, 1988), pp. 1–82.
[89] M. Jean and J.-J. Moreau, in *Proceedings of Contact Mechanics International Symposium*, edited by A. Curnier (Presses Polytechniques et Universitaires Romandes, Romandes, Switzerland, 1992), pp. 31–48.
[90] J. J. Moreau, in *Powders and Grains*, edited by C. Thornton (Brookfield, Rotterdam, 1993), pp. 227–232.
[91] J. J. Moreau, Eur. J. Mech. A/Solids **13**, 93 (1994).
[92] J. J. Moreau and M. Jean, in *Engineering Systems Design and Analysis*, edited by A. Lagarde and M. Raous (American Society of Mechanical Engineering, New York, 1996), pp. 201–208.
[93] H. J. Herrmann and S. Luding, Continuum Mech. Thermodyn. **10**, 189 (1998).
[94] A. W. Lees and S. F. Edwards, J. Phys. C **5**, 1921 (1972).
[95] D. J. Evans and G. P. Morriss, Phys. Rev. A **30**, 1528 (1984).
[96] D. J. Evans and G. P. Morriss, *Statistical Mechanics of Nonequilibrium Liquids* (Academic Press, London, 1990).
[97] M. Babic, Int. J. Eng. Sci. **35**, 523 (1997).
[98] B. J. Glasser and I. Goldhirsch, Phys. Fluids **13**, 407 (2001).
[99] H. Hayakawa, Phys. Rev. E **61**, 5477 (2000).
[100] M. Alam and S. Luding, J. Fluid Mech. **476**, 69 (2003).
[101] I. Goldhirsch and N. Sela, Phys. Rev. E **54**, 4458 (1996).
[102] R. Larson, *The Structure and Rheology of Complex Fluids* (Oxford University Press, New York, 1999).
[103] M. L. Falk, J. S. Langer, and L. Pechenik, Phys. Rev. E **70**, 011507 (2004).
[104] S. Ogawa, in *Proceedings of the US-Japan Seminar on Continuum Mechanical and Statistical Approaches in the Mechanics of Granular Materials*, edited by S. Cowin and M. Satake (Gakujutsu Bunken Fukyu-Kai, Tokyo, 1978), pp. 208–217.
[105] V. Garzó and J. W. Dufty, Phys. Rev. E **59**, 5895 (1999).
[106] M. L. Falk, Phys. Rev. B **60**, 7062 (1999).
[107] J. S. Langer, Phys. Rev. E **64**, 011504 (2001).
[108] J. S. Langer and L. Pechenik, Phys. Rev. E **68**, 061507 (2003).
[109] S. Kobayashi, K. Maeda, and S. Takeuchi, Acta Metall. **28**, 1641 (1980).
[110] K. Maeda and S. Takeuchi, Philos. Mag. A **44**, 643 (1981).
[111] D. Srolovitz, K. Maeda, and T. Egami, Philos. Mag. A **44**, 847 (1981).
[112] S. Takeuchi and K. Maeda, Key Eng. Mater. **13–15**, 749 (1987).
[113] D. Deng, A. S. Argon, and S. Yip, Philos. Trans. R. Soc. London, Ser. A **329**, 549 (1989).
[114] A. Argon and H. Kuo, Mater. Sci. Eng. **39**, 101 (1979).
[115] A. Argon and L. Shi, Acta Metall. **31**, 499 (1983).
[116] A. Lemaître, Phys. Rev. Lett. **89**, 195503 (2002).
[117] A. Lemaître, e-print cond-mat/0206417.
[118] A. Lemaître, e-print cond-mat/0307216, *Lecture Notes in Physics* (Springer, Berlin, in press).
[119] A. Lemaître and J. Carlson, Phys. Rev. E **69**, 061611 (2004).